PERGAMON

International Journal of Multiphase Flow 27 (2001) 673–683

International Journal of Multiphase Flow

www.elsevier.com/locate/ijmulflow

Turbulence structure over a particle roughness

Ryoichi Kurose [1], Satoru Komori *

Department of Mechanical Engineering, Kyoto University, Kyoto 606-8501, Japan

Received 25 January 2000; received in revised form 30 July 2000

Abstract

The effect of particle roughness on turbulence structure in a water boundary layer in an open channel flow is experimentally investigated using a laser-Doppler velocimeter (LDV). As a wall boundary, a fixed- or a free-particle wall is used against various particle-occupation densities ε. The results show that for the same ε the friction velocity on the fixed-particle wall is larger than that on the free-particle wall, and that both friction velocities have maxima in the region of $0.1 \leqslant \varepsilon \leqslant 0.2$. The Reynolds stress and turbulence intensities outside the roughness sublayer, normalized by the friction velocity, are independent of the particle roughness. The u–v quadrant decomposition technique elucidates that ejection events are superior to sweep events in the vicinity of the wall over smooth and free-particle walls, whereas over the fixed-particle wall the sweep events are more dominant in the production of the Reynolds stress than the ejection events.

Keywords: Particle roughness; Turbulence structure; Similarity

1. Introduction

Turbulence structure in a rough-wall turbulent boundary layer has been an important subject in many environmental and industrial studies for predicting the particle dispersion in the atmospheric boundary layer and for designing particle-transportation equipment and so on.

Nakagawa and Nezu (1977) were the first to study turbulence structure over a fixed-particle wall, where spherical particles with diameters of 1–13 mm were most-closely fixed on the smooth wall. They showed that the Reynolds stress and turbulence intensities become larger for the rough particle boundary than for the smooth boundary and that sweep events are more superior to

* Corresponding author.

E-mail address: komori@mech.kyoto-u.ac.jp (S. Komori).

[1] Present address: Yokosuka Research Laboratory, Central Research Institute of Electric Power Industry (CRIEPI), Kanagawa 240-0196, Japan.

0301-9322/01/$ - see front matter
PII: S0301-9322(00)00044-6

ejection events as the surface roughness increases. Rashidi et al. (1990) and Kaftori et al. (1995a,b, 1998) also measured the turbulence quantities and particle motions in an open channel flow with many free particles moving over the smooth wall. Rashidi et al. (1990) showed that particles of small diameters less than 0.12 mm decrease both the Reynolds stress and turbulence intensities, whereas the large particles of diameters more than 1.1 mm increase them. Thus, the turbulence structure is strongly influenced by both the fixed and free particles, but the difference in the effects of the fixed and free particles has not yet been studied. Moreover, the effects of the ratio of the occupied area of particles projected on the bottom wall to the total bottom area (hereafter referred to as particle-occupation density ε) on the turbulent structure have not been clarified.

On the other hand, Perry and Abell (1977), Raupach (1981), Perry et al. (1987), Acharya and Escudier (1987) and Krogstad et al. (1992) measured the turbulence quantities in the turbulent boundary layer over the mesh-screen roughness. They examined whether the Townsend's Reynolds-number similarity hypothesis, representing that for sufficiently large Reynolds-number turbulent motions are independent of the wall roughness outside the roughness sublayer (Townsend, 1976; Perry and Abell, 1977), is valid or not. If the hypothesis is valid, the distributions of the turbulence quantities normalized by the wall shear stress should be essentially the same between smooth and rough surfaces (Acharya and Escudier, 1987). From the measurements of the Reynolds stress and spectra of velocity fluctuations by means of a hot-wire anemometry, Krogstad et al. (1992) concluded that the turbulent motions depend on the surface conditions and therefore the similarity hypothesis is not held. However, the roughness of the mesh-screen used there is extremely steep, and the effects of the mesh-screen on the turbulence structure may not be the same as those of the particle roughness.

In this paper, we aim to investigate the effects of the particle roughness on the turbulence structure over the fixed or free-particle beds with various particle-occupation densities ε, and to examine the validity of the Townsend's similarity hypothesis. As will be mentioned later, the free particles used here are transported downstream without being lifted up, and thereby we refer this type of roughness as free-particle wall hereafter. Instantaneous streamwise and vertical water velocities are simultaneously measured using a two-color laser-Doppler velocimeter (LDV), and the organized turbulent motions near the particle walls are visualized using a hydrogen-bubble technique.

2. Experiment

Fig. 1 shows the experimental apparatus and measuring system. The apparatus used was a glass open flume 7 m long, 0.5 m wide and 0.2 m deep, and the fresh water was recirculated into it through a head tank (see Komori et al., 1989). A fully developed turbulent flow was established in the region beyond 3 m downstream from the inlet of the flume.

The experimental conditions are listed in Table 1, where $\overline{Uc}$ is the cross-sectional mean velocity, u^* the friction velocity, ε the particle-occupation density and d^+ is the dimensionless particle diameter defined by du^*/ν with the kinematic viscosity ν. As a bottom wall boundary, a smooth wall (case A), a fixed-particle wall (case B) or a free-particle wall (case C) was used. The particles used were the glass beads with 4 mm diameter and 2620 kg/m^3 density. In the case B, the particles were arranged in a staggered form on the smooth wall. In the case C, the particles were provided into

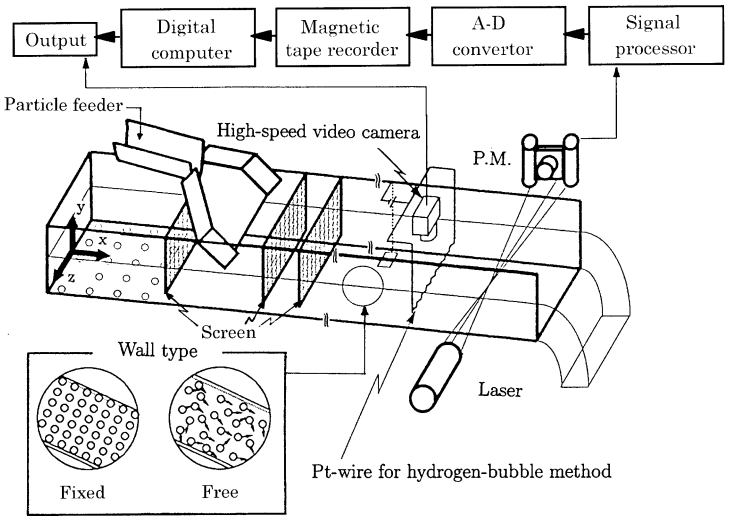

Fig. 1. Schematic diagram of experimental apparatus and measuring instruments.

Table 1
Experimental conditions

Case	Wall type	$\overline{Uc}$ (cm/s)	u^* (cm/s)	ε (dimensionless)	d^+ (dimensionless)
A	Smooth	35.6	1.89	0	–
B1	Fixed-particle	30.1	2.75	0.0437	98.2
B2	Fixed-particle	29.6	3.00	0.0873	107
B3	Fixed-particle	28.1	3.11	0.175	111
B4	Fixed-particle	28.2	2.93	0.349	105
B5	Fixed-particle	28.3	2.81	0.698	100
B6	Fixed-particle	29.3	2.45	0.907 (max)	87.5
C1	Free-particle	34.1	2.20	0.0561	78.6
C2	Free-particle	33.4	2.25	0.0805	80.4
C3	Free-particle	33.2	2.45	0.122 (limit)	87.5

the open flume from a particle feeder equipped in the upstream region and transported downstream on the bottom smooth wall without both forming the streaks and being lifted up associated with the organized turbulence motion (see Rashidi et al., 1990). The case B6 corresponded to the case where the particles were most closely fixed on the bottom wall with the maximum particle-occupation density of $\varepsilon = 0.907$. The case C3 had a maximum number of particles where the free particles can move on the smooth bottom wall without being stuck and the steady flow condition can be established. In order to remove the disturbance effect by particles dropping from the feeder on the flow structure, three screens were mounted at the distance of $x = 0.2$, 0.5 and 0.6 m from the inlet of the flume. The u^* was estimated by extrapolating the vertical distribution of the Reynolds stress $-\overline{uv}$ for $y/\delta \geqslant 0.2$ to the wall

$$\frac{-\overline{uv}}{u^{*2}}\Big|_{y/\delta=0} = 1. \tag{1}$$

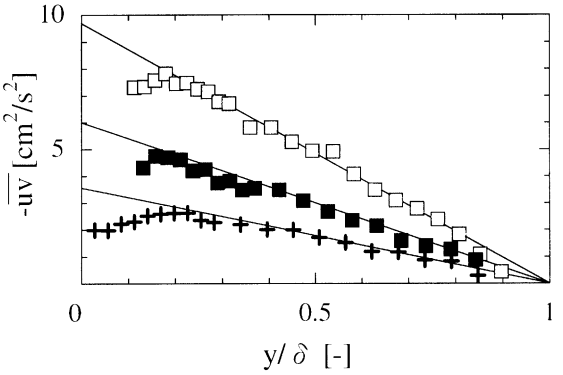

Fig. 2. Typical distributions of the Reynolds stress: + case A; □ case B3; ■ case C3.

The typical vertical distributions of $-\overline{uv}$ are shown in Fig. 2. The Reynolds-number based on $\overline{Uc}$ and flow depth δ, $Re(=\delta\overline{Uc}/\nu)$, was 11 250 for all cases.

Instantaneous streamwise and vertical water velocities were simultaneously measured at $x=4.8$ m on the centreline ($z=0$) by using a two-color laser-Doppler velocimeter (LDV, DANTEC 55X). The measuring point was vertically traversed up from the elevation of 1 mm above the smooth wall for the case A and from the elevation of 5 mm above the smooth wall (1 mm above the top surface of particles) for the cases B and C. The sampling interval and size were 0.0002 s and 900 000, respectively.

The organized turbulent motions over the particle walls were visualized using a hydrogen-bubble technique. A platinum wire of 40 μm diameter was set parallel to the flume floor at $y^+(=yu^*/\nu)=10$. The bubble streaks were viewed from the free surface side and recorded at an interval of 0.005 s by a high-speed video system (NAC HSV-400).

3. Results and discussion

3.1. Friction velocity and mean velocity profile

Fig. 3 shows the variations of the friction velocity normalized by that for the smooth wall, u^*/u_s^*, against the particle-occupation density ε. The u^*/u_s^* for the fixed-particle wall (case B) is larger than that for the free-particle wall (case C) at the same ε. This is attributed to the fact that the relative velocity between particles and fluid in the vicinity of the wall is smaller for free particles than that for fixed particles, and the larger relative velocity generates a stronger turbulence. The cases B and C have maximum values of u^*/u_s^* at almost the same ε in the range of $0.1\leqslant\varepsilon\leqslant0.2$, although the maximum value for the case C corresponds to the limited value of $\varepsilon=0.122$. This suggests that a saturated state for the friction stress is attained in this range.

The u^*/u_s^* over the fixed-particle wall with the maximum particle-occupation density of $\varepsilon\approx0.9$ is plotted against the dimensionless particle diameter d^+ in Fig. 4 together with the previous measurements by Nakagawa and Nezu (1977) and Kurose and Komori (1995). The u^*/u_s^* is roughly proportional to d^+ independent of the fluid (air or water), and the relation is given by

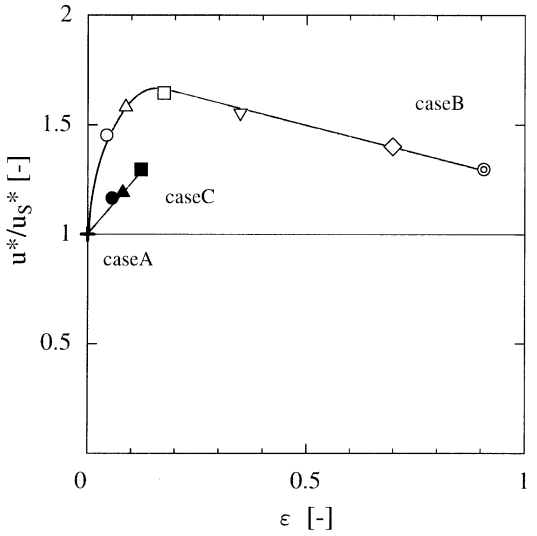

Fig. 3. Relationship between friction velocity and particle-occupation density: + case A; ○ case B1; △ case B2; □ case B3; ▽ case B4; ◇ case B5; ◎ case B6; ● case C1; ▲ case C2; ■ case C3.

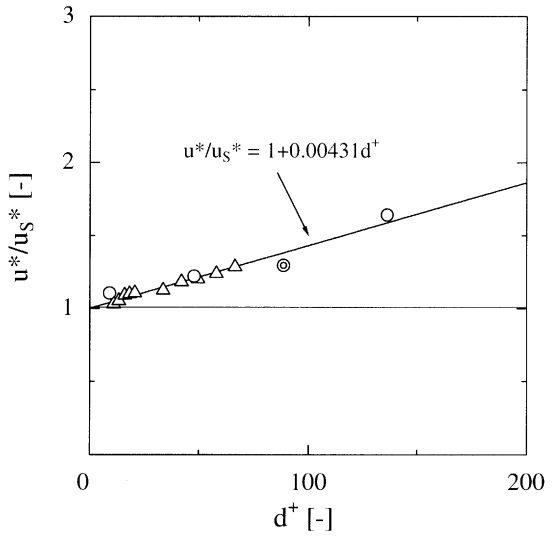

Fig. 4. Correlation between friction velocity at $\varepsilon \approx 0.9$ and dimensionless particle diameter: ○ in the air flow (Kurose and Komori, 1995); △ in the water flow (Nakagawa and Nezu, 1977); ◎ in the water flow (case B6).

$$\frac{u^*}{u_s^*} = 1 + 0.00431\, d^+. \tag{2}$$

This means that the friction velocity u^* for the fixed-particle wall with the maximum $\varepsilon(\approx 0.9)$ can be estimated from the friction velocity for the smooth wall u_s^* and dimensional particle diameter d^+.

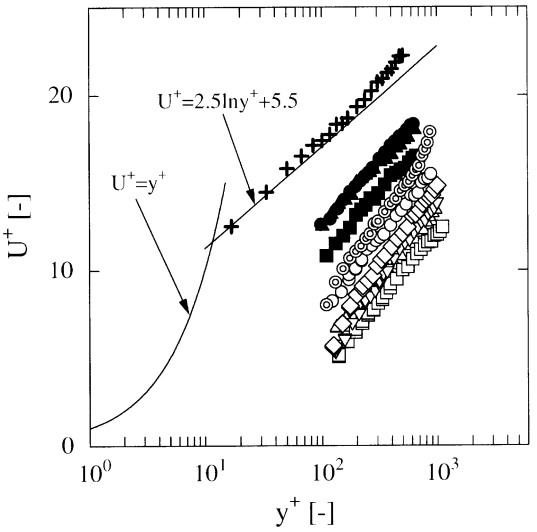

Fig. 5. Mean velocity profiles over smooth and rough particle walls. Symbols as in Fig. 3.

The distributions of the mean velocity normalized by u^*, $U^+(=\overline{U}/u^*)$ are shown against the dimensionless wall unit $y^+(=yu^*/\nu)$ in Fig. 5. The profile for the smooth wall (case A) is in good agreement with the empirical expressions indicated by solid lines in the figure. The profiles for the particle walls (cases B and C) shift downward with almost the same inclination.

3.2. Reynolds stresses, turbulence intensities and spectra

Figs. 6 and 7 show the vertical distributions of the Reynolds stress, $-\overline{uv}$, turbulence intensities, $u'(=\sqrt{\overline{u^2}})$ and $v'(=\sqrt{\overline{v^2}})$, and Reynolds stresses from the second and fourth quadrants (see Fig. 8), $\overline{uv}_2$ and $\overline{uv}_4$, normalized by u^*. The $\overline{uv}_2$ and $\overline{uv}_4$ are obtained using the u–v quadrant decomposition technique of Willmarth and Lu (1972) and Lu and Willmarth (1973), such that

$$\overline{uv}_i = \lim_{T\to 0}\frac{1}{T}\int_0^T uvI\,\mathrm{d}t, \tag{3}$$

$$I = \begin{cases} 1 & \text{if } |uv|_i \geqq Hu'v', \\ 0 & \text{otherwise.} \end{cases}$$

The hyperbolic hole of size H was set to 2.0 for all cases to select only the strong ejection and sweep events, as shown in Fig. 9. Fig. 10 shows the spectra and co-spectra of u and v, S_u, S_v and Co_{uv}, normalized by u^* and y, at $y/\delta = 0.1$ and 0.5 for the cases A, B3 and C6. The S_u, S_v and Co_{uv} are defined by

$$\int_0^\infty S_u\,\mathrm{d}k_1 = \overline{u^2}, \quad \int_0^\infty S_v\,\mathrm{d}k_1 = \overline{v^2}, \quad \int_0^\infty Co_{uv}\,\mathrm{d}k_1 = -\overline{uv}, \tag{4}$$

where $k_1(=2\pi f/\overline{U}$, f: the frequency, $\overline{U}$: the local mean velocity) is the one-dimensional wave number.

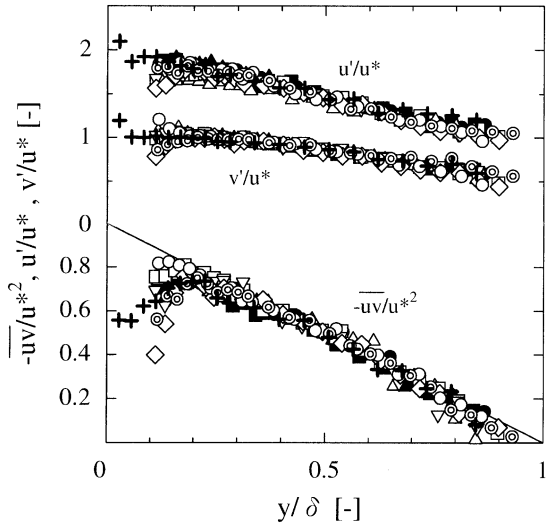

Fig. 6. Vertical distributions of the Reynolds stress and turbulence intensities. Symbols as in Fig. 3.

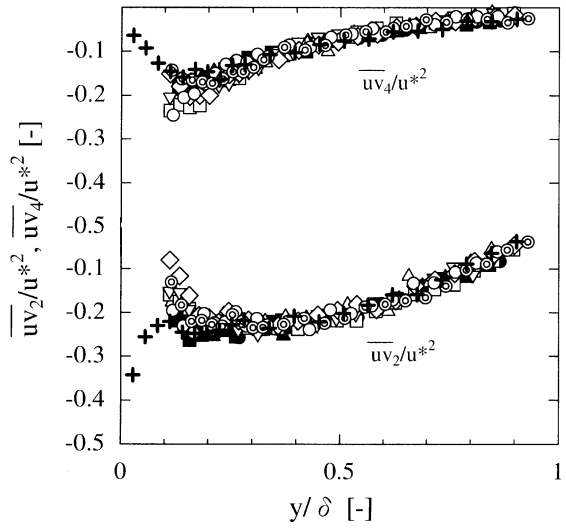

Fig. 7. Vertical distributions of the Reynolds stresses from the second and fourth quadrants. Symbols as in Fig. 3.

In the outer region of $y/\delta \geqslant 0.2$, where the flow is not directly influenced by the particle roughness, the distributions of the turbulence intensities, the Reynolds stress and the spectra in Figs. 6, 7 and 10(b) almost coincide with each other independent of the type of the particle roughness. This supports the Townsend's Reynolds-number similarity hypothesis (Townsend, 1976; Perry and Abell, 1977). The hypothesis represents that for sufficiently large Reynolds numbers turbulent motions are independent of the wall roughness outside the roughness sublayer, and implies that the distributions of the turbulence quantities normalized by the wall shear stress

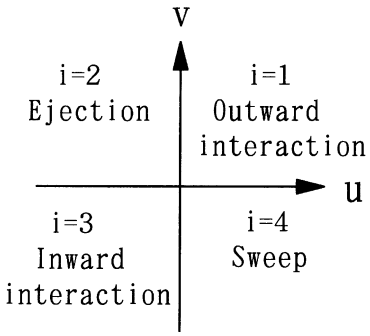

Fig. 8. The u–v quadrant decomposition technique.

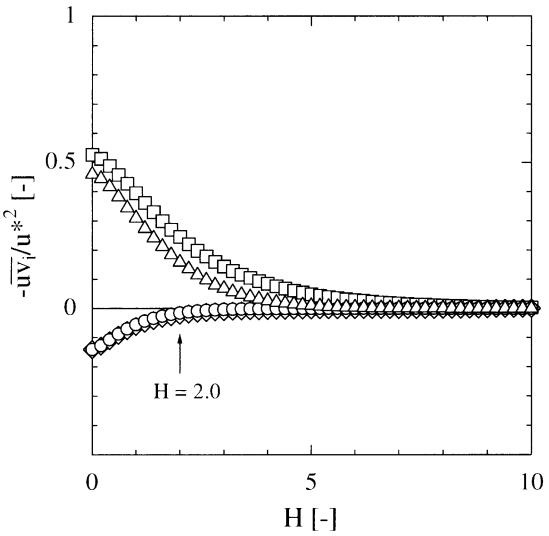

Fig. 9. Contributions to the Reynolds stress from the four quadrants: ◇ quadrant 1; □ quadrant 2; ○ quadrant 3; △ quadrant 4.

(friction velocity) should be essentially the same between smooth and rough surfaces. Krogstad et al. (1992), who investigated the turbulence quantities such as the Reynolds stress, turbulence intensities and spectra in the turbulent boundary layer on the mesh-screen, concluded that these turbulence quantities depend on the nature of the surface and that the Townsend's similarity hypothesis is not held. In fact, they showed that the distributions of v' and S_v on the mesh-screen are significantly larger than those on the smooth wall. This suggests that the Townsend's Reynolds-number similarity hypothesis is not held essentially for the steep roughness, but for the particle roughness with a gentle geometry, the similarity is attained as shown in the present measurements.

Also, the comparisons of S_u, S_v and Co_{uv} for $y/\delta = 0.1$ in Fig. 10(a) show that the distributions of the spectra over the smooth and particle walls roughly coincide with each other independent of roughness even in the vicinity of the wall and suggests that the weak roughness like particle walls

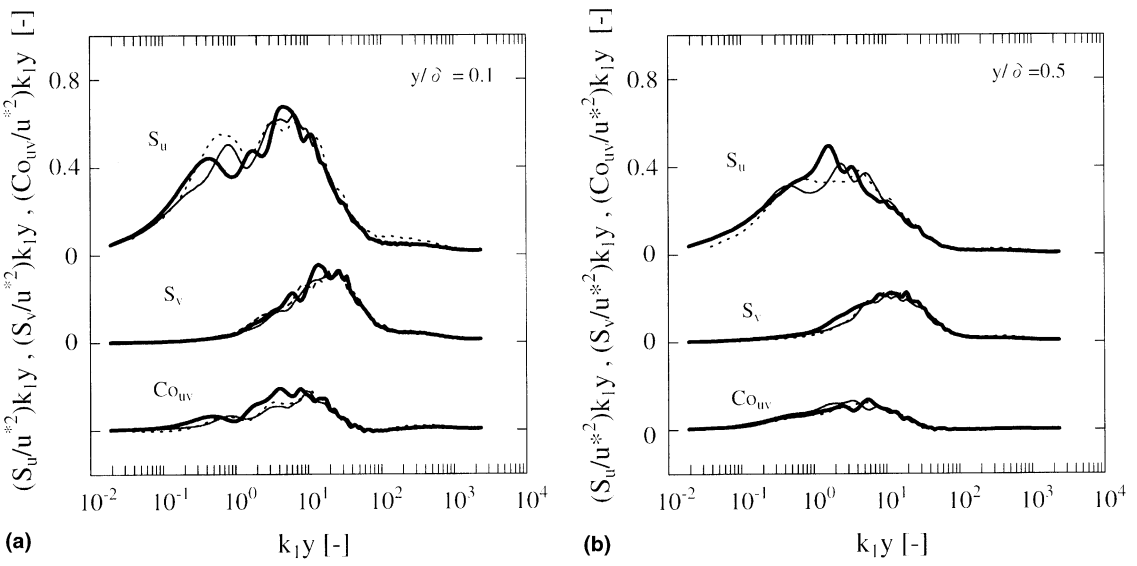

Fig. 10. Spectra and co-spectra: (a) at $y/\delta = 0.1$; (b) at $y/\delta = 0.5$; - - - case A; ▬ case B3; —— case C3.

hardly affects the spectra. In contrast with the present result, the spectra over the mesh-screen roughness are known to be quite different from those over the smooth wall (Krogstad et al., 1992).

On the other hand, the absolute value of $\overline{uv}_2$ decreases and that of $\overline{uv}_4$ increases as the roughness increases in the vicinity of the wall. The trends are compared well with Nakagawa and Nezu (1977) and Krogstad et al. (1992). Fig. 11 shows the vertical variations of the ratio of $\overline{uv}_2$ to

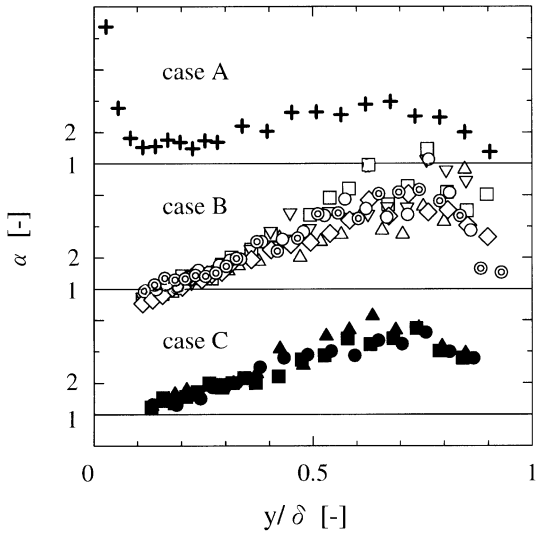

Fig. 11. Vertical distributions of the ratio of the contribution of ejection to the Reynolds stress and to that of sweep. Symbols as in Fig. 3.

$\overline{uv}_4$, $\alpha(=\overline{uv}_2/\overline{uv}_4)$ for the three cases. The production of $\overline{uv}$ in the vicinity of the wall is dominated by ejection events ($\alpha > 1$) for the smooth and free-particle walls (cases A and C), whereas the contribution of sweep events increases ($\alpha < 1$) for the fixed-particle walls (case B).

In order to visualize the organized turbulent motion near the particle wall, a hydrogen-bubble technique was used. It was observed that the dimensionless average space between the low-speed streaks, $\lambda^+(=\lambda u^*/\gamma)$ was 119.6 for the case B6, which was about 20% larger than that of $\lambda^+ = 99.0$ for the case A. Further, the number of visible strong ejection events associated with the low-speed streaks obviously decreased for the particle walls, compared to the smooth wall. This suggests that the strong turbulence produced by the roughness breaks the low-speed streaks and decreases the number of ejection events. Also, the break up is considered to be more effective for the fixed-particle wall than for the free-particle wall since the relative velocity between particle and fluid near the wall is larger for the fixed-particle wall than for the free-particle.

4. Conclusions

The effect of particle roughness on the turbulence structure in the turbulent boundary layer was experimentally investigated. As the particle roughness, the fixed-particle and free-particle walls with several particle-occupation densities were used. The main results from this study can be summarized as follows.

1. For the same particle-occupation density ε, the friction velocity for the fixed-particle wall is larger than that for the free-particle wall. Both the friction velocities have the maximum values in the saturation region of $0.1 \leqslant \varepsilon \leqslant 0.2$. Beyond the saturation region, the free particles moving on the smooth wall begin to be stuck on the wall.
2. The friction velocity for the fixed-particle wall with the maximum particle-occupation density can be estimated by the empirical formula (2).
3. When the Reynolds stress, turbulence intensities and spectra in the outer region are normalized by the friction velocity, the normalized quantities for the smooth and rough particle walls coincide with each other independent of the type of the particle roughness. This supports the Townsend's Reynolds-number similarity hypothesis.
4. The production of the Reynolds stress is dominated by ejection events in the vicinity of the smooth and free-particle walls, whereas the contribution of sweep events becomes large for the fixed-particle wall.

Finally, since the data presented here are only limited to fixed values of the Reynolds-number, particle size and particle density, important questions still remain unanswered as to why and on what condition the friction velocity over the particle wall has a maximum, over what kind of roughness the similarity is attained, and so on. To answer the questions, further experiments for various flow-and roughness-conditions will be required.

Acknowledgements

This work was supported by the Japan Ministry of Education, Science and Culture through Grants-in-Aid (No. 11450077).

References

Acharya, M., Escudier, M., 1987. Turbulent flow over mesh roughness. In: Turbulent Shear flow 5, Springer, Berlin, pp. 176–185.

Kaftori, D., Hetsroni, G., Banerjee, S., 1995a. Particle behavior in the turbulent boundary layer. I. Motion, deposition, and entrainment. Phys. Fluids 7, 1095–1106.

Kaftori, D., Hetsroni, G., Banerjee, S., 1995b. Particle behavior in the turbulent boundary layer. II. Velocity and distribution profiles. Phys. Fluids 7, 1107–1121.

Kaftori, D., Hetsroni, G., Banerjee, S., 1998. The effect of particles on wall turbulence. Int. J. Multiphase Flow 24, 359–386.

Komori, S., Murakami, Y., Ueda, H., 1989. The relationship between surface-renewal and bursting motions in an open-channel flow. J. Fluid Mech. 203, 103–123.

Krogstad, P.-A., Antonia, R.A., Browne, L.W.B., 1992. Comparison between rough- and smooth-wall turbulent boundary layers. J. Fluid Mech. 245, 599–617.

Kurose, R., Komori, S., 1995. Relationship between particle motion and turbulence structure in turbulent boundary layer flow over particle-rough wall. Trans. Jpn. Soc. Mech. Eng. 61, 1693–1700 (in Japanese).

Lu, S.S., Willmarth, W.W., 1973. Measurements of the structure of the Reynolds stress in a turbulent boundary layer. J. Fluid Mech. 60, 481–571.

Nakagawa, H., Nezu, I., 1977. Prediction of the contributions to the Reynolds stress from bursting events in open-channel flows. J. Fluid Mech. 80, 99–128.

Perry, A.E., Abell, C.J., 1977. Asymptotic similarity of turbulence structure in smooth- and rough-walled pipes. J. Fluid Mech. 79, 785–799.

Perry, A.E., Lim, K.L., Henbest, S.M., 1987. An experimental study of the turbulence structure in smooth- and rough-wall boundary layers. J. Fluid Mech. 177, 437–466.

Rashidi, M., Hetsroni, G., Banerjee, S., 1990. Particle-turbulence interaction in a boundary layer. Int. J. Multiphase Flow 16, 935–949.

Raupach, M.R., 1981. Conditional statistics of Reynolds stress in rough-wall and smooth wall turbulent boundary layers. J. Fluid Mech. 108, 363–382.

Townsend, A.A. (Ed.), 1976. The Structure of Turbulent Shear Flow. Cambridge University Press, Cambridge, pp. 139–143.

Willmarth, W.W., Lu, S.S., 1972. Structure of the Reynolds stress near the wall. J. Fluid Mech. 54, 39–48.